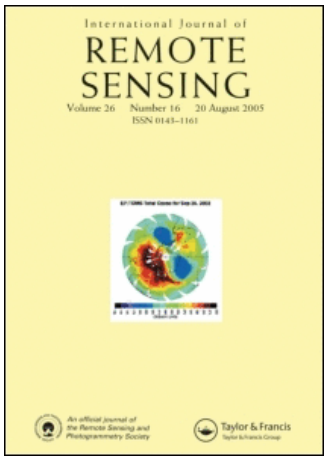

International Journal of Remote Sensing
Publication details, including instructions for authors and subscription information:
http://www.informaworld.com/smpp/title~content=t713722504

Extracting structural characteristics of herbaceous floodplain vegetation under leaf-off conditions using airborne laser scanner data

To cite this Article: Straatsma, M. and Middelkoop, H. , 'Extracting structural characteristics of herbaceous floodplain vegetation under leaf-off conditions using airborne laser scanner data', International Journal of Remote Sensing, 28:11, 2447 - 2467
To link to this article: DOI: 10.1080/01431160600928633
URL: http://dx.doi.org/10.1080/01431160600928633

International Journal of Remote Sensing
Vol. 28, No. 11, 10 June 2007, 2447–2467

Extracting structural characteristics of herbaceous floodplain vegetation under leaf-off conditions using airborne laser scanner data

M. STRAATSMA* and H. MIDDELKOOP
Department of Physical Geography, Utrecht University, PO Box 80115, 3508 TC Utrecht, The Netherlands

(*Received 24 March 2006; in final form 2 June 2006*)

Hydrodynamic models of river flow need detailed and accurate friction values as input. Friction values of floodplain vegetation are based on vegetation height and density. To map spatial patterns of floodplain vegetation structure, airborne laser scanning is a promising tool. In a test for the lower Rhine floodplain, vegetation height and density of herbaceous vegetation were measured in the field at 42 georeferenced plots of 200 m^2 each. Simultaneously, three airborne laser scanning (ALS) surveys were carried out in the same area resulting in three high resolution, first pulse, small-footprint datasets. The laser data surveys differed in flying height, gain setting and laser diode age. Point density of the laser data varied between 10 and 75 points m^{-2}. Point heights relative to the DTM derived from the ALS data were used in all analyses. Laser points were labelled as either vegetation or ground using three different methods: (1) a fixed threshold value; (2) a flexible threshold value based on the inflection point in the point height distribution; and (3) using a Gaussian distribution to separate noise in the ground surface points from vegetation. Twenty-one statistics were computed for each of the resulting vegetation-point distributions, which were subsequently compared with field observations of vegetation height. Additionally, the percentage index (PI) was computed to relate density of vegetation points to hydrodynamic vegetation density. The vegetation height was best predicted by using the inflection method for labelling and the 95 percentile as a regressor (R^2=0.74–0.88). Vegetation density was best predicted using the threshold method for labelling and the PI as a predictor (R^2=0.51). The results of vegetation height prediction were found to depend on the combined effect of flying height, gain setting or laser diode age. The quality of the estimation of vegetation height and density is also affected by point density, for densities lower than 15 points m^{-2}. We conclude that high resolution ALS data allows to estimate vegetation height and density of herbaceous vegetation in winter condition, but field reference data remains necessary for calibration.

1. Introduction

In response to the increased awareness of the socio-economic importance of river flooding in the past decades, considerable effort has been undertaken in recent years to develop hydrodynamic models of overbank flow to predict extreme flood water

*Corresponding author. Email: m.straatsma@geo.uu.nl

International Journal of Remote Sensing
ISSN 0143-1161 print/ISSN 1366-5901 online © 2007 Taylor & Francis
http://www.tandf.co.uk/journals
DOI: 10.1080/01431160600928633

levels for the design of flood defence structures. The hydrodynamic roughness of the floodplain surface is one of the key parameters of these models, and depends on vegetation structure. The role of vegetation roughness in hydrodynamic modelling is becoming increasingly important to assess the implications of ecological rehabilitation measures in floodplain areas for overbank flow patterns and extreme water levels. This is because ecological rehabilitation may involve considerable changes in floodplain vegetation, and may lead to a more extensive use of floodplains, resulting in complex patterns and succession stages of floodplain vegetation (Baptist *et al.* 2004, Jesse 2004, Van Stokkom *et al.* 2005). Although various schemes have been developed to represent vegetation roughness in two- and three-dimensional hydrodynamic models, and numerous flume experiments have been reported to determine vegetation roughness, there is still considerable lack of quantitative estimates of vegetation patterns and inherent roughness of real floodplains (Darby 1999, Fischer-Antze *et al.* 2001, Stoesser *et al.* 2003, Nicholas and McLelland 2004). Therefore, monitoring floodplain vegetation structure becomes essential for accurately modelling the hydrodynamics of submerged floodplains (Mason *et al.* 2003). Key parameters used in numerical two- or three-dimensional modelling schemes to calculate hydrodynamic roughness of vegetation are vegetation height and density, average stem spacing and flexural rigidity (Kouwen and Li 1980, Klopstra *et al.* 1997). Vegetation density is the projected plant area in the direction of the flow per unit volume. For cylindrical vegetation, this equals the product of number of stems or stalks per unit area multiplied by the average stem diameter (Fischer-Antze *et al.* 2001, Wilson and Horrit 2002). Numerous models have been presented to convert vegetation structural characteristics to roughness (i.e. Kouwen and Li 1980, Klopstra *et al.* 1997, Baptist 2005).

Traditional methods to map vegetation patterns within the floodplain are based on visual interpretation and manual classification of vegetation units from aerial photographs, as applied for the lower Rhine floodplains (Jansen and Backx 1998, Van Velzen *et al.* 2003). These, however, may become inadequate to monitor the spatio-temporal dynamics of vegetation roughness, since the procedures are time consuming and do not allow documentation of within-class variation of vegetation roughness. There is thus a need for a faster and more adequate approach to assess hydrodynamic roughness of vegetated floodplain surfaces. In case of the River Rhine in the Netherlands, such an approach has to be specifically suited for herbaceous vegetation since these occupy the largest floodplain areas (Duel *et al.* 2001).

For many years, successful attempts have been reported to map vegetation types using multispectral or hyperspectral remote sensing data (Ringrose *et al.* 1988, Mertes *et al.* 1995, Thompson *et al.* 1998, Schmidt and Skidmore 2003, Van der Sande *et al.* 2003, Rosso *et al.* 2005). Recently, spectral information has been combined with height information in classification schemes (e.g. Hill *et al.* 2002, Ehlers *et al.* 2003). Mertes (2002) gives an overview of different aspects of remote sensing of riverine landscapes. The resulting maps with vegetation classes need to be converted to a vegetation structure map using a lookup table, since vegetation structure cannot be extracted directly from the spectral image. In the classification procedure, spatial detail of vegetation structural characteristics is lost. In contrast, airborne laser scanning (ALS) provides information on the distribution of vegetation directly, and therefore has been used extensively in forestry surveys to estimate forest characteristics (Lefsky *et al.* 2002, Lim *et al.* 2003). It has been

used to map vegetation height of floodplains as well, but only in summer when vegetation was in leaf-on condition (Cobby *et al.* 2001, Mason *et al.* 2003). However, in the Netherlands, most floods occur in winter (Middelkoop and Van Haselen 1999). Relations derived for summer vegetation may therefore be unrepresentative.

The main goal of this study was to estimate vegetation height and density of herbaceous floodplain vegetation in senescence on a field plot level using airborne laser scanning data. Flexural rigidity and average stem spacing seems unlikely to be extractable from ALS data in case of herbaceous vegetation. We focused on herbaceous vegetation, as this is the dominant vegetation type in Dutch floodplains. Three different methods to distinguish between ground points and vegetation points were evaluated. We determined a large number of statistical characteristics of the vegetation points and evaluated which of these were the best predictors of vegetation height and density. The study was based on ALS data collected during three surveys in different sections of the lower Rhine floodplain in the Netherlands: one in March 2001 and two in March 2003. Simultaneously with each laser survey, field reference data were collected on vegetation height and density at the same floodplain sections.

2. Extraction of vegetation structure of low vegetation from ALS data

ALS has been extensively used for various applications, such as aerodynamic roughness determination (Menenti and Ritchie 1994), ice sheet modelling (Krabill *et al.* 2000), and coastal dune morphology (Woolard and Colby 2002). It has been successfully applied to measure vegetation structure (Wehr and Lohr 1999). In forestry, laser scanning has been successfully applied to map forest properties, such as timber volume (Naesset 1997), tree height (Naesset 2002, Brandtberg *et al.* 2003) or number of stems and stem diameter (Lefsky *et al.* 1999, Naesset 2004). Lim *et al.* (2003) give an overview of airborne laser scanning of forests.

Only a few papers have reported on documenting and mapping vegetation height of low vegetation. Weltz *et al.* (1994) and Ritchie *et al.* (1996) found good correspondence between field data and airborne laser measurements of plant height, canopy cover and ground cover of low height rangeland vegetation. However, they did not present regression models to estimate these parameters from laser data. Davenport *et al.* (2000) and Cobby *et al.* (2001) used low-resolution (1 point per $9\,m^2$) laser data to estimate crop height. Since the vegetation density of the crops was very high, they were unable to detect the ground surface in the laser data, and therefore they used the standard deviation of de-trended laser heights as a predictor. The standard deviation of laser scan height data correlated in a (log–) linear way with crop height determined by field sampling ($R^2=0.89$ in Davenport *et al.* 2000, $R^2=0.80$ in Cobby *et al.* 2001). Hopkinson *et al.* (2004) predicted vegetation height of shrubs, aquatic marshland vegetation, grassland and herbs. Like the previous studies, they used the standard deviation of all laser points, corrected for local ground surface undulations, as a predictor of vegetation height ($R^2=0.77$). All laser data and field data were collected during leaf-on season. The parameters in the regression models in these studies varied greatly. Cobby *et al.* (2001) used a log–linear regression, which did not give satisfactory results on the data of Hopkinson *et al.* (2004). Moreover, the slope of the regression reported by Hopkinson *et al.* (2004) was three times higher than the one from Davenport *et al.* (2000). The high regression slope reported by Davenport *et al.* (2000) might be due to higher density

of the crops when compared with the natural vegetation studied by Hopkinson *et al.* (2004). Dense crops create a continuous canopy cover and most laser pulses will reflect off the top of the canopy, thereby limiting the variation in the vertical distribution.

In spite of this successful application of ALS laser data to document vegetation height of crops and marshlands in summer, it remains to be evaluated whether these methods are applicable for assessing vegetation structure in Dutch floodplains, when vegetation is leafless, and only the stalks of the grasses and herbs are present. Thus, contrary to Davenport *et al.* (2000) and Cobby *et al.* (2001), the vegetation type to be mapped is very open and consists of thin stalks. Consequently, regression models established in these previous studies might not be valid for winter vegetation. Besides vegetation height, vegetation density is also needed as input to hydrodynamic models. No literature was found that related laser-derived parameters to the vegetation density of herbaceous vegetation.

3. Materials and methods

3.1 *Study area*

This study is based on laser data collected in three floodplain sections of the distributaries of the River Rhine in The Netherlands: 'Duursche Waarden' floodplain (DW) along the right bank of the River IJssel, and the 'Afferden en Deestse Waarden' (ADW) and the 'Gamerense Waarden' (GW) floodplains along the left bank of the River Waal (figure 1). In all these floodplains, landscaping measures have been carried out to reduce flood levels and to restore the ecology. For these floodplains, high-density laser data were acquired by the Dutch Ministry of Transport, Public Works and Water Management as a monitoring pilot. Vegetation presently consists of hardwood and softwood forest and shrubs, but is dominated by herbaceous vegetation. Vegetation is characterized by a heterogeneous pattern of vegetation types and structure. Herbaceous vegetation consists mostly of sedge (*Carex hirta L.*), sorrel (*Rumex obtusifolius L.*), nettle (*Urtica dioica L.*), thistle (*Cirsium arvense L.*) and clover (*Trifolium repens L.*). The vegetation height inside the plots ranged between 0.26 and 1.66 m.

3.2 *Field measurements*

We measured vegetation height and density in 42 field plots of homogeneous vegetation (figure 1): 12 plots in the DW and ADW floodplain in March 2001, and 30 plots in the GW floodplain in March 2003. The plots represented a large range of herbaceous vegetation types. Plot size was at least 200 m^2, to ensure a sufficient number of laser points available for subsequent analysis. The plots were geo-located using a Garmin GPS12, resulting in a horizontal accuracy of 5 m, which is the estimated positioning error (EPE) given by the Garmin proprietary software. Vegetation height was measured in two steps: (1) we estimated the average vegetation height as an imaginary plane through the average top of the vegetation and (2) we measured the length of 30 randomly selected stalks reaching at least half the height of step 1. The mean and standard deviation of the 30 measured heights were registered. Vegetation density was determined from the product of the number of stalks per unit area and the average stalk diameter, which was based on the same 30 stalks using a sliding gauge.

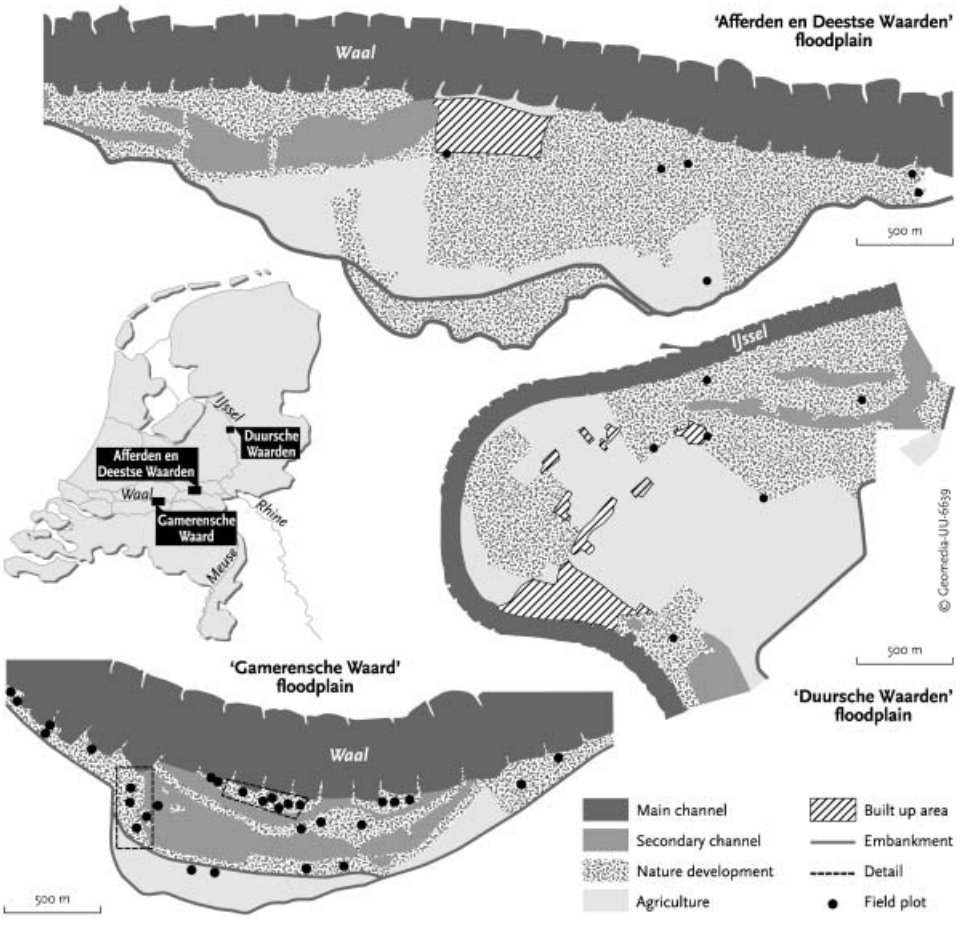

Figure 1. Location of the study sites and field plots.

3.3 *Airborne laser scanning data*

The laser data were acquired by Fugro-Inpark using the FLI-MAP II system mounted on a helicopter (Huising and Gomes Pereira 1998, Baltsavias 1999a). FLI-MAP, fast laser imaging and mapping airborne platform, is a scanning laser range finder combined with a dGPS and an inertial navigation system for positioning. An overview of the laser scanning technique used is given by Wehr and Lohr (1999). FLI-MAP has an additional option to change the gain setting. The gain is the amount of amplification of the return signal before it is converted to a digital signal. Surveyors may increase the gain to compensate for the declining emission of energy due to ageing of the laser diode.

Table 1 summarizes the characteristics of the three laser scanning campaigns and the locations are shown in figure 1. The laser data collected in 2001 in the 'Duursche Waarden' and the 'Afferdensche en Deestse Waarden' floodplains is referred to as the 'DWADW' dataset. Between 2001 and 2003, Fugro-Inpark added a second laser range finder to FLI-MAP, resulting in a doubling of the data collection rate and a re-orientation of the scanners. Instead of one nadir looking scanner, the two scanners were facing 7° forward and backwards to decrease the number of

Table 1. Metadata for the three laser scanning campaigns.

Acquisition time	Floodplain location	Scan angle	Number of sensors	Sensor age	Flying height	Gain	Point density	Flight strips
March 2001	DWADW	$\pm 30^{\circ}$	1	old	80 m	100%	12	Single
March 2003a	GWhigh	$\pm 30^{\circ}$	2	new	80 m	80%	75	Double
March 2003b	GWlow	$\pm 30^{\circ}$	2	new	55 m	100%	60	Single

occlusions in built-up areas. With the new FLI-MAP configuration two datasets were collected in the 'Gamerense Waard' floodplain in 2003. One was acquired from a height of about 80 m and with normal gain setting of the receiver, resulting in the 'GWhigh' dataset, the second from a minimum height of 55 m and with the maximum gain, called the 'GWlow' dataset. The GWhigh dataset covers the entire GW floodplain, while each flight line was flown twice to increase the point density resulting in a point density of 75 points m^{-2}. The GWlow dataset only covers 10 field plots (figure 1). The three datasets enable the evaluation of the resulting regression equations to estimate vegetation height, which are influenced by the different flight parameters (table 1).

3.4 *DTM extraction and labelling*

For the determination of the vegetation height, the effect of the undulations of the terrain should be eliminated. This can be done by constructing a digital terrain model (DTM) based on points that are expected to represent the ground. This is the common practice, as reported in most literature. Sithole and Vosselman (2004) give an overview of eight different DTM extraction methods. They conclude that all methods perform well in relatively flat terrain such as lowland river floodplains.

3.4.1 DTM filtering. For this study, only the laser points that were located inside the field plots were considered. For each plot, a DTM was constructed using iterative residual analysis based on a simplified version of the method of Kraus and Pfeifer (1998). In each step, a surface was computed as a local second order trend surface in a moving window. The window radius was 1.5 m to ensure enough points are available for a robust fit. A larger window would lead to a loss of detail. The residual distance to this surface was computed for each point. Points with positive residuals are likely to be vegetation points. Since the range of values for an unvegetated, flat surface was computed and proved to be approximately 30 cm, a simple weight function was applied to compute the surface in the next iteration: points with an residual value of more than 15 cm were excluded from further analysis in the DTM processing. With the remaining points a new DTM surface was computed. Iterations were continued until all points had residuals less than 15 cm. The final DTM was a smooth surface running through the middle of these ground points. Heights relative to the DTM were used in subsequent computations.

3.4.2 Vegetation labeling. In a second step, a detailed study was carried out to decide which points should be labelled as vegetation. Three different methods were evaluated: (1) a threshold method; (2) an inflection method; and (3) a Gaussian method. The first method is based on a fixed threshold value above the DTM; the

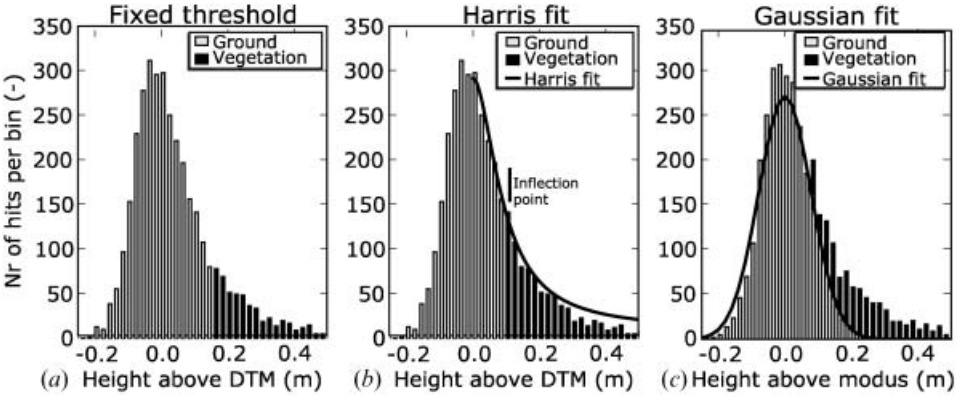

Figure 2. Labelling of vegetation point (black bars) and ground points (grey bars); (*a*) threshold value of 0.15 m; (*b*) inflection point; and (c) difference between Gaussian fit and point distribution.

other two are based on histogram analysis of heights above the DTM. For the threshold method, we used 15 cm above the DTM as a threshold (figure 2a), similar to the DTM filtering setting.

For the second and third method laser points were binned in 2 cm vertical bins. Narrower bin intervals led to very spiky histograms, and wider intervals to a loss of detail. The vertical point distribution was considered as a combination of a noise distribution of ground points and a uniform distribution of vegetation points. The inflection method finds the point of maximum concave-up curvature in the upper limb of the histogram, the so-called inflection point. The rationale behind the selection of this point as a threshold value is that the sum of a noise distribution of the ground points and the uniform distribution of the vegetation points gives a strong concave up curvature. Any point that lies above the inflection point value is labelled as a vegetation point, all points below are ground points. To find the inflection point, a Harris function was fitted through the upper part of the histogram for each field plot (figure 2b). The Harris function is defined as:

$$y(h) = (a + bh^c)^{-1} \tag{1}$$

where $y(h)$ is the frequency of occurrence in a bin at height h. Parameters a, b and c are estimated from a least squares fit using a minimum of 15 bins to ensure stability of the fit. The inflection point was obtained by determining the height at which the second derivative of the Harris function reaches the maximum value. The height of the inflection point in the example is 0.09 m (figure 2b).

The Gaussian method fits a Gaussian curve to the histogram. The Gauss curve is defined as:

$$p(h) = (2\pi\sigma)^{-0.5} \exp\left(-\frac{1}{2}\left(\frac{h-\mu}{\sigma}\right)^2 \right) \tag{2}$$

where $p(h)$ is the frequency of noise occurrence at height h, μ is the mean and σ is the standard deviation. Fitting the Gauss curve boils down to finding the mean and

standard deviation of the *ground points*. The mean of all points in the plot, however, also considers the vegetation points. Therefore, we used the mode of the distribution instead of the mean to estimate μ. The disadvantage of the mode is that the data have to be binned, which introduces a dependence on the choice of the bin boundaries. Moreover, the mode can be undetermined. To counteract this effect we used the *weighted mode*, the average of the seven most frequent values in the point distribution, weighed by frequency. The standard deviation was based on the points lower than the weighted mode using the 15.9 and 25 percentiles. These two standard deviations were averaged to derive the final standard deviation. The Gauss curve was then scaled by the product of twice the number of observations below the weighted mode and the bin width (figure 2c). The difference between the histogram values and the fitted Gauss curve in the range above one standard deviation above the mode provided the number of points per bin that were assumed to represent vegetation. In each bin, points were labelled randomly as vegetation up to the predicted number of vegetation points. This ensured a spatially random distribution of the vegetation points.

3.5 *Relative point height distribution and comparison with field data*

The three methods, described in the previous section, result in three height distributions of vegetation points for each plot. With respect to predicting the vegetation height, each point distribution was described by 21 different statistics:

- central tendency: mean, median, mode;
- variability: standard deviation and variance;
- shape: skewness and kurtosis;
- percentiles: D_{10}, D_{20}, …, $D_{100} + D_{95}$, D_{96}, D_{97}, D_{98}, D_{99}.

The observed vegetation heights in the field were subsequently compared with these statistics using correlation as an indicator of the strength of the relation. Forward stepwise linear regression was subsequently carried out to determine the strongest predictors (Wonnacott and Wonnacott 1990). The effects of gain setting and flying height were tested using two statistical tests; a *t*-test on differences in means and a paired sample *t*-test of the D_{95} percentiles of the GWhigh and GWlow data set. Samples could be paired for these datasets since the same reference plots were used. To gain insight in the effect of laser diode age and the flight parameters, the slopes of the regression models for vegetation height were compared using a single percentile as a regressor using three Student's *t*-tests.

Vegetation density was predicted using the percentage index (*PI*), which computes the percentage of laser hits that fall within the height range of the vegetation (h_1 to h_2):

$$PI_{h_1-h_2} = \frac{1}{h_2 - h_1} * \frac{N_{h_1-h_2}}{N_{\text{tot}}} \tag{3}$$

in which $N_{h_1-h_2}$ is the number of vegetation points between height 1 and 2 above the ground surface, N_{tot} is the total number of points in the field plot including vegetation points and ground surface points. The height interval for PI is equal to the height of the vegetation. The first term in the equation is added, because higher vegetation would increase $N_{h_1-h_2}$, but does not necesserily increase the vegetation

Table 2. Field measurements of vegetation height and density.

Floodplain	Plot no.	Hv[b]	Dv[c]	Floodplain[a]	Plot no.	Hv[b]	Dv[c]
GW	1	0.69	0.12	GW	35	0.59	0.046
GW	3	0.55	0.088	GW	36	0.91	0.084
GW	7	0.99	0.13	GW	37	0.81	0.034
GW	9	0.66	0.113	GW	39	0.57	0.048
GW	10	0.48	0.015	GW	41	1.66	0.015
GW	11	0.44	0.22	GW	42	0.43	0.065
GW	12	0.77	0.35	GW	45	0.38	0.025
GW	13	0.50	0.082	GW	47	0.30	0.020
GW	15	0.38	0.070				
GW	16	0.84	0.16	ADW	21	1.34	0.20
GW	17	0.69	0.091	ADW	22	0.61	0.17
GW	18	0.70	0.077	ADW	23	0.76	0.72
GW	19	1.18	0.12	ADW	31	0.42	0.037
GW	20	1.49	0.15	ADW	32	0.38	0.0054
GW	23	0.26	0.11	ADW	33	0.30	0.027
GW	24	0.84	0.34				
GW	26	0.73	0.29	DW	21	0.72	0.065
GW	27	0.90	0.067	DW	22	0.70	0.049
GW	29	0.47	0.025	DW	23	0.75	0.0003
GW	31	0.47	0.016	DW	31	0.39	0.011
GW	32	0.52	0.018	DW	32	0.47	0.0020
GW	33	0.71	0.060	DW	33	0.49	0.032

[a]GW="Gamerense Waard" floodplain; ADW="Afferden en Deestse Waarden" floodplain; DW="Duursche Waarden" floodplain.
[b]Hv=vegetation height (m).
[c]Dv=vegetation density ($m^2\,m^{-3}$).

density. Ideally, h_1 should be set to zero, and h_2 to the maximum height of the vegetation. However, h_1 should not include noise of the ground surface. Therefore we chose the lower limit of the vegetation point height distribution as a minimum value.

4. Results

4.1 *Field measurements of vegetation height and density*

Vegetation height in the 42 sample plots ranged from 0.26 to 1.66 m. Vegetation density varied between 0.0003 and 0.72 $m^2\,m^{-3}$. Table 2 gives the full list of the data collected in the field plots.

4.2 *Estimation of vegetation height and density from laser data*

Figure 3 shows a three-dimensional scatter plot of the laser scanning representation of the herbaceous vegetation shown on the photograph. The laser points in this image were labelled using the inflection method. For each plot, the three different labelling methods were applied, threshold, inflection point and Gaussian fit, which resulted in three vegetation point distributions per plot. Each distribution was described by the 21 laser-derived statistics and the *PI* parameter. For each individual dataset (DWADW, GWhigh, GWlow), the correlations between the field vegetation heights and the laser statistics were computed. The average correlation per labelling method and per laser-derived statistics is shown

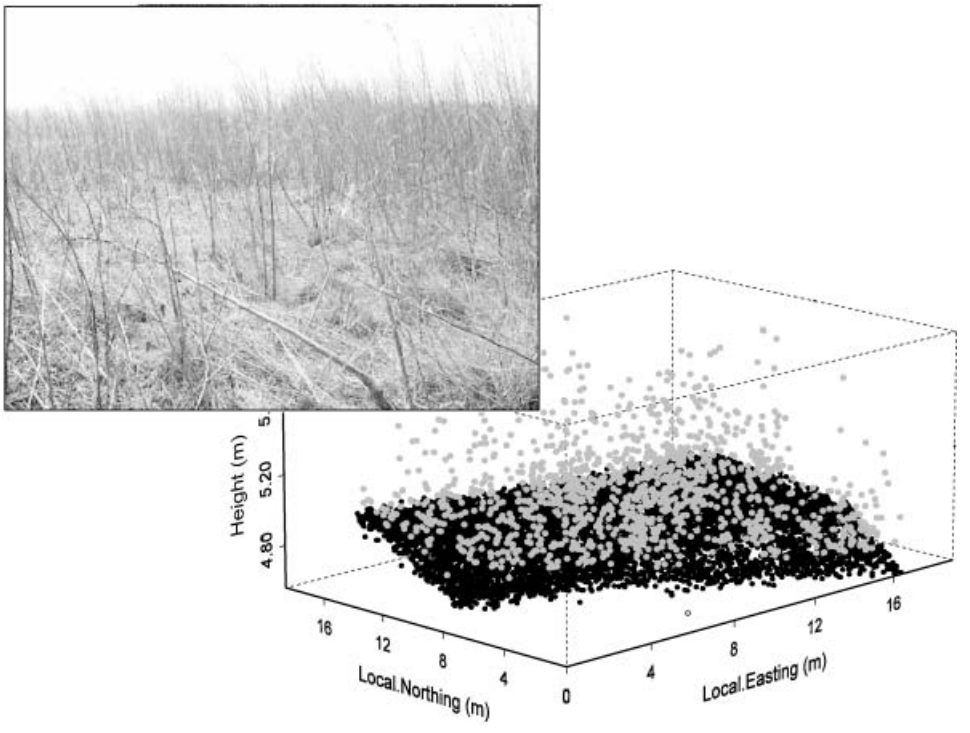

Figure 3. Three-dimensional laser data scatter plot of the herbaceous vegetation on the picture. Vegetation points depicted in grey, ground points in black

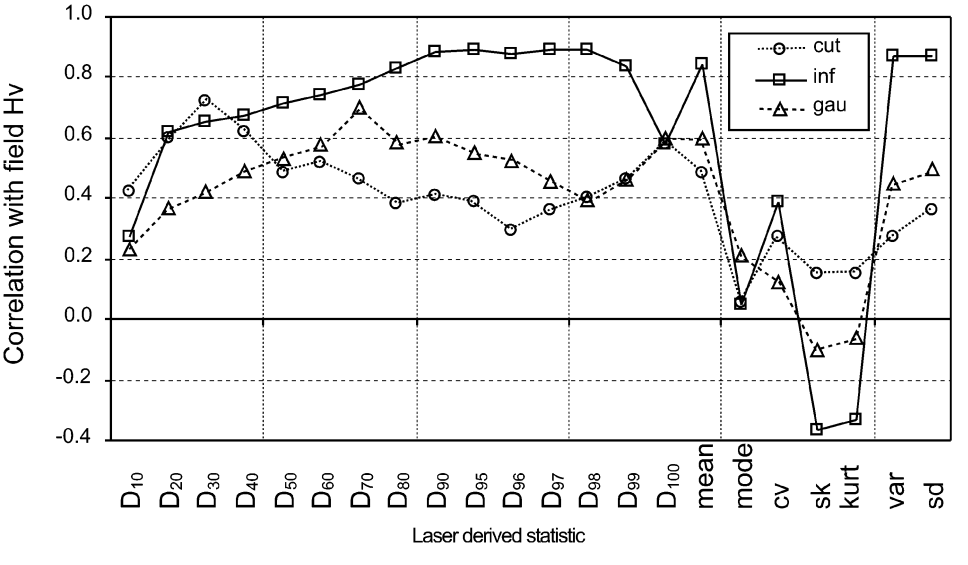

Figure 4. Effect of point labelling methods on the strength of correlation between laser-derived statistics and field vegetation heights. $D_x = X$ percentile of the vegetation points; cv=coefficient of variation; sk=skewness; kurt=kurtosis; var=variance; sd=standard deviation.

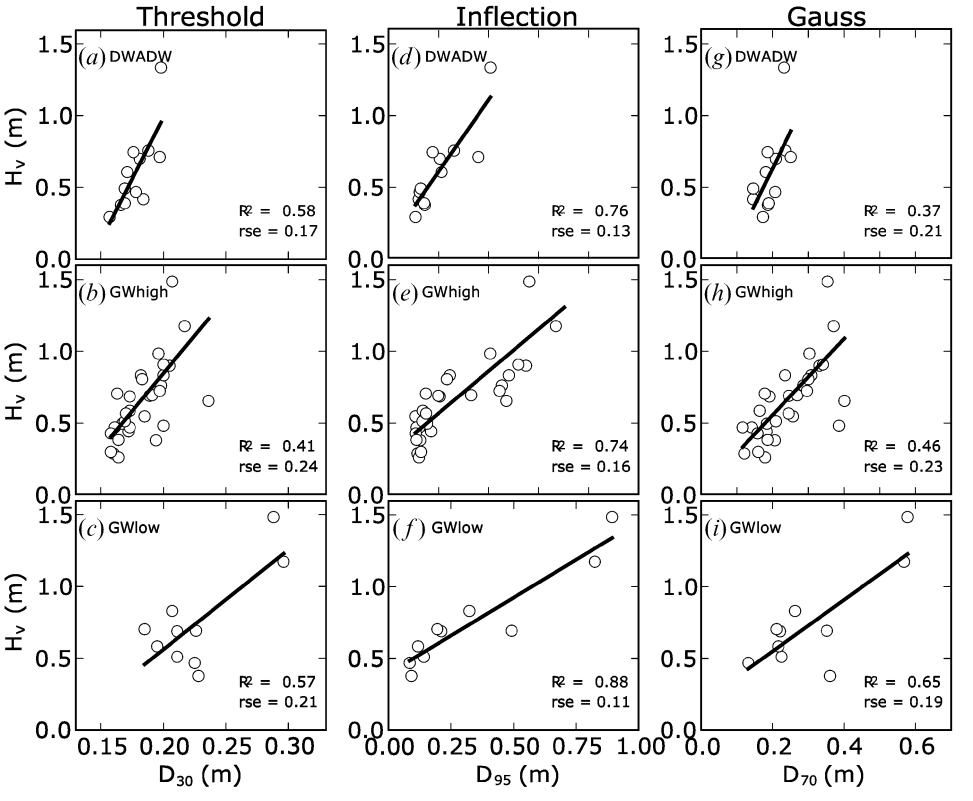

Figure 5. Scatter plots of predictions of vegetation height per dataset using three different point labelling methods: (*a*), (*b*) and (*c*) threshold method; (*d*), (*e*) and (*f*) inflection method; (*g*), (*h*) and (*i*) Gaussian method

in figure 4. The following parameters showed the highest correlations: (1) D_{30} for the threshold method (r=0.72); (2) D_{90} to D_{98} plus the standard deviation and variance for the inflection method (r>0.85); and (3) D_{70} for the Gaussian fit (r=0.70).

The parameter with the highest correlation was chosen for vegetation height prediction for each labelling method. For the inflection method, a few parameters showed a high correlation. The 95 percentile was selected to maintain congruency in predictors even though the standard deviation and the variance showed a marginally better correlation coefficient. Figure 5 shows nine scatter plots depicting the measured vegetation heights vs the predicted heights based on the selected laser percentiles. Forward stepwise regression was carried out to select the best regression model, starting with the selected percentile (D_{30}, D_{95}, and D_{70} for the threshold, inflection and Gaussian method respectively). This did not result in the selection of any additional parameters for any of the regression models, due to multicollinearity constrictions. Table 3 summarizes the regressions.

Results of the prediction of vegetation density using the *PI* are shown as scatter plots (figure 6). The threshold and Gaussian method show a positive relation with vegetation density (R^2=0.51 and 0.49, respectively). Conversely, prediction based on the inflection labelling shows a weak negative relation (R^2=0.09). Table 4 summarizes the equations.

Table 3. Regression equations for vegetation height.

Labelling method	Dataset	Regression equation	R^2	RSE (m)[a]
Threshold				
	DWADW	$Hv=17.20D_{30}-2.45$	0.58	0.17
	GWhigh	$Hv=10.57D_{30}-1.26$	0.41	0.24
	GWlow	$Hv=6.98D_{30}-0.83$	0.57	0.21
Inflection				
	DWADW	$Hv=2.51D_{95}+0.11$	0.76	0.13
	GWhigh	$Hv=1.47D_{95}+0.28$	0.74	0.16
	GWlow	$Hv=1.06D_{95}+0.40$	0.88	0.11
Gaussian				
	DWADW	$Hv=5.13D_{70}-0.39$	0.37	0.21
	GWhigh	$Hv=2.67D_{70}+0.02$	0.46	0.23
	GWlow	$Hv=1.80D_{70}+0.19$	0.65	0.19

[a] Residual standard error.

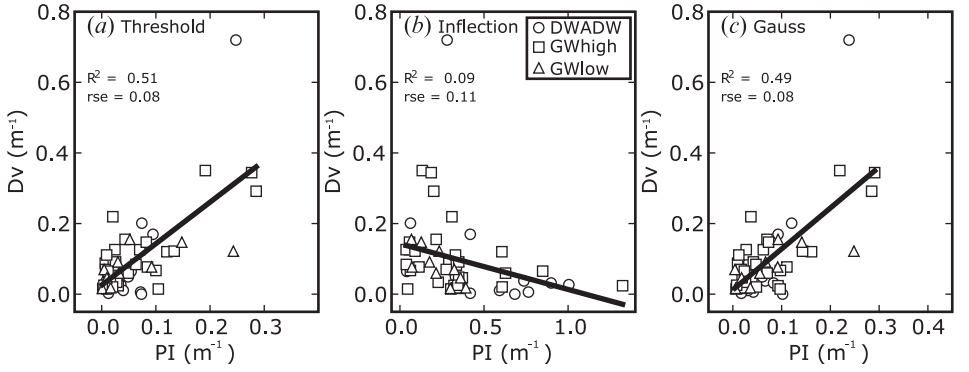

Figure 6. Scatter plots of predictions of vegetation density per dataset using three different point labelling methods: (*a*) threshold method; (*b*) inflection method; and (*c*) Gaussian method.

4.3 *Effect of point density*

To investigate the effect of varying the point density on the estimation of vegetation height and density, the analyses were repeated for the GWlow dataset that was progressively thinned out. The original point density of 60 points m^{-2} was step-wise reduced to create 12 different datasets with 50, 40, 30, 20, 15, 10, 8, 6, 4, 2, 1 and 0.5 points m^{-2}. Point density was reduced by omitting data points at regular intervals from the original dataset, which was in chronological order of data aquisition. This mimics the spatial distribution that would be obtained from a higher flying speed or

Table 4. Regression equations for vegetation density using three different methods.

	Regression equation	R^2	RSE (m^{-1})[a]
Threshold	$Dv=1.18PI+0.03$	0.51	0.08
Inflection	$Dv=-0.13PI+0.14$	0.09	0.11
Gaussian	$Dv=1.16PI+0.01$	0.49	0.08

[a] Residual standard error.

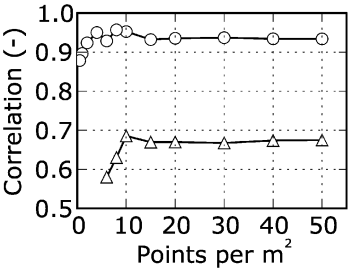

Figure 7. Effect of point density on correlation strength for vegetation height (D_{95} in ○) and density (*PI* in Δ). No variation in correlation is present at point densities higher than 15 points m^{-2}.

altitude, with an equal footprint size. For each of the thinned datasets, the D_{95} percentile was calculated using the inflection labelling method and subsequently correlated with observed vegetation height. The *PI* was based on the threshold method and correlated to the vegetation density. No correlation could be computed for the vegetation density for point densities lower than 6 points m^{-2} as no vegetations points occurred at some plots. Figure 7 shows the effect of decreasing point density on the correlation coefficient between the D_{95} percentile of the laser data and vegetation height plus the correlation between the *PI* and vegetation density as measured in the field. In general, correlations obtained using low point densities are lower (r=0.85 for vegetation height), but remarkably, correlations do not change for point densities of 15 points m^{-2} or higher. Apparently, a point density of 15 points m^{-2} is most efficient for vegetation height and vegetation density mapping in this study area and for this size of field plots.

4.4 *Effect of flying altitude and gain setting*

The GWhigh and GWlow laser datasets share 10 field plots, which allowed to compare the combined effect of lower flying altitude and increased the gain setting (cf. table 1). The following tests were performed using the inflection labelling method and the D_{95} percentile. A t-test on differences in means of both data sets showed no significant difference between the D_{95} percentiles of the GWhigh and GWlow dataset (α=90%, p=0.54). These results were in accordance with expectations, since the difference in the average value of the D_{95} percentiles was expected to be low relative to the range of vegetation heights. In contrast, a *paired sample* t-test did reveal significant differences between the height of the D_{95} percentile of the GWhigh and GWlow datasets (α=90%, p=0.08). These results indicate that a low flying height, combined with a high gain, improves detection of the top of the vegetation.

The slope of the regression lines between laser data and observed vegetation height also indicates the ability of the laser signal to detect the top of the vegetation. A steeper slope indicates a poorer detection of the vegetation top. Figure 5 shows the regression lines for the DWADW, GWhigh and the GWlow data sets. The slope of the DWADW is steepest, and the slope of the GWlow dataset is mildest. Three Student's t-tests were carried out to determine whether there were significant differences between the slopes of the regression lines based on vegetation labelling using the inflection method. All differences in slope were significant at the 95% level of confidence. Table 5 gives the significance levels of the three t-tests.

Table 5. Confidence levels of Student's *t*-tests on difference in slopes of regression lines.

	DWADW GWhigh	GWhigh
GWhigh	99.9	
GWlow	99.9	95

5. Discussion

5.1 *DTM and point labelling*

The DTMs for all plots, created using the method of Kraus and Pfeifer (1998), did not show any outliers, and created a smooth surface. Based on visual inspection, the DTMs of the plots seemed very typical of the gently undulating topography observed in the field. However, as Kraus and Pfeifer (1998) stated, it will smooth out terrain jumps, such as erosive river banks. Sithole and Vosselman (2004) also note in their filtering algorithm test that discontinuities in the terrain surface poses one of the largest problems in point cloud filtering. In case floodplain-wide mapping of vegetation structure is needed, this effect should be taken into account. In this research, laser points from a single dataset, but from different flight strips were combined into one dataset per plot. Height differences between flight strips were checked visually for a few plots, but no systematic errors were detected. Moreover, the combined point distributions did not show a bimodal distribution for any plot. Still, it is advised to create a DTM based on individual flight strips.

Point labelling was done based on the heights relative to the DTM. The three different methods show a varying level of flexibility with respect to discrimination between vegetation and ground points. The threshold method, with the threshold set to 15 cm above the DTM is the most rigid, and identical to the method the DTM was created. It assumes that no vegetation points are present below 15 cm above the DTM. The advantage with this method is that point labelling is possible on a per-point base. The other two methods need a histogram of the point distribution. Both assume that the peak in the point distribution represents the ground surface, an assumption that is not violated in case of herbaceous floodplain vegetation in winter condition. The inflection method defines a threshold value based on the shape of the height histogram as characterized by the Harris function. This function has three fit parameters [a, b, c; equation (1)], which introduces flexibility with respect to height and width of the point distribution. The height of the inflection point was in all cases lower than 15 cm, and typically around 5 cm. The assumption that underlies this method, is that the ground and vegetation points together generate a point of maximum inflection in the histogram. The disadvantage of this method is that it will also label points as vegetation at sites where no vegetation occurs. The Gaussian method assumes that the ground points show a Gaussian distribution, and labels points as vegetation whenever their frequency in a certain bin exceeds the frequency of the Gaussian distribution. The Gaussian curve [equation (2)] in our case depends on the standard deviation and the weighted mode of the ground points. The number of points labelled as vegetation differ per method. The threshold method labels least points as vegetation, the inflection method most, which is related to the percentile used in the regressions. For example, the inflection method labels most points as vegetation, and therefore a high percentile, D_{95}, correlates best with vegetation height.

5.2 *Vegetation height and density estimation*

Vegetation height of herbaceous floodplain vegetation can be predicted reliably at the plot level using high-density first-pulse airborne laser scanning data (R^2=0.74–0.88 using the inflection labelling method), while estimation of vegetation density is less accurate (R^2=0.51 using the threshold method). The inflection method shows the best predictions of vegetation height for all three datasets (figure 5). The threshold and the Gaussian method in general selected fewer points, and are therefore more sensitive to outliers in the height distribution. These outliers might result from the relatively low spatial accuracy of the plot boundaries, which was about 5 m. This could have led to the inclusion of laser hits related to other vegetation types. Conversely, vegetation density was predicted better by the threshold and Gaussian method (figure 6). The PI relates point density of vegetation points to hydrodynamic vegetation density. The inflection method labels more points as vegetation than the two other methods, but the PI values did not correlate well with field reference values, and are even negatively correlated. This could be caused by the height at which the vegetation density was measured in the field, which was at least at 13 cm above the ground surface (half the minimum vegetation height). This is well above a typical inflection height of 5 cm. The threshold method performed marginally better than the Gaussian method. The inverse dependence of *PI* on $h2$ minus $h1$ [equation (3)] could lead to unrealistic values in case $h2$ nears or equals $h1$. This should not be a problem for vegetation higher than 25 cm as in this study.

5.3 *Comparison with other research*

In this paper we predicted vegetation height and density of low herbaceous vegetation in winter condition, consisting of open vegetation that generates a weak return. Nevertheless, the quality of prediction of vegetation height in this study is similar to the results obtained in regression models for forests: Means *et al.* (1999), Naesset (2002) and Naesset and Bjerknes (2001) reported regression models explaining 74–95% of the variance in the field reference data of vegetation height. Given the small range in height of herbaceous floodplain vegetation, it is remarkable that the results obtained in our study are of similar quality as those obtained in forestry surveys.

Davenport *et al.* (2000), Cobby *et al.* (2001), and Hopkinson *et al.* (2004) studied vegetation height of low vegetation under leaf-on condition. However, in our study, we predicted vegetation height of herbs in senescence. This means that the vegetation signal is much weaker, due to the smaller plant surface. Still, the predictive quality of vegetation height found in this study is comparable to the studies on low vegetation under leaf-on condition. The differences found in the regression equations from this study and previous studies (Davenport *et al.* 2000, Cobby *et al.* 2001, Hopkinson 2004) demonstrate that portability of the derived relations is low. It points to the need for future field reference data and more physical understanding of these relations.

No studies on vegetation density of low vegetation are known to the authors. We chose to relate the vegetation density to the percentage index (R^2=0.51 using the threshold method) because of the rationale that denser and higher vegetation should result in more vegetation points in the laser datasets. Although prediction results could be somewhat increased by including percentiles as additional regressors, we

chose not to as percentiles refer to height. Laser-derived parameters from forestry studies that relate to vegetation density, such as stem number and stem diameter explained 39–85% of the total variance (Lefsky *et al.* 1999, Naesset 2002). Similar to our study, forestry studies obtained better results for vegetation height than for parameters related to vegetation density.

5.4 *Effects of flight parameters; flying height, laser diode age and gain setting*

Detection of vegetation by laser scanning depends on many factors related to the minimum detectable object (Baltsavias 1999b). Flight parameters for this study are given in table 1. The results showed that airborne laser scanning is well able to predict the height of senescent herbaceous vegetation, in a height range order of 0.2–2 m (table 3). The average stalk diameter of 4 mm of the herbaceous floodplain vegetation apparently exceeds the minimum detectable object size.

The DWADW and GWhigh data sets yielded different slopes of the regression models to estimate vegetation height, which was significant at the 99.9 confidence level (table 5). The reason for this difference might be the age of the laser diode age, the calibration settings or the larger average incidence angle in the GWhigh dataset, due to the reorientation of the laser scanners between 2001 and 2003. The slope of the GWlow dataset was significantly steeper than for the GWhigh dataset. The paired sample *t*-test also showed significant differences between the GWhigh and GWlow datasets. Remarkably, the increase in the regression slope of the GWhigh and GWlow dataset was significant even though the field and laser data were collected on the same day. The reason for the difference in slope and 95 percentile must therefore be the combination of the reduced flying height and increased gain setting for the GWlow dataset. Together these effects result in a larger amount of energy reaching the analogue to digital converter in the laser scanner from an equally reflective object. Consequently, small objects are detected better, and the regression slopes are lower. With these datasets, it is impossible to assess the influence of the individual parameters. However, as long as the parameters influencing the regression equations are unclear, field reference data will remain necessary to establish the regressions.

Naesset (2004) concluded for spruce and pine forest that the effect of flying altitude is marginal and that the flying altitude can be increased by 60% without any serious effect on the estimated stand properties. Nilsson (1996) mentions that optimal laser footprint size for forest surveys changes only with acquisition season. These conclusions for forests are contrary to our conclusions for herbaceous floodplain vegetation. The reason for this difference might lie in the shape and structural properties of the vegetation involved. Trees are larger and Naessets data were collected in leaf-on conditions, which makes detectability of trees better than thin floodplain herbs, which seem at the edge of detectability.

The remaining unexplained variance might result from measurement uncertainties or location errors in the field data. Although the field plots comprised 200 m^2 of homogeneous vegetation each, a 5 m positional error in the location of the plots may influence the height distribution due to spatial heterogeneity of floodplain vegetation. Another source of unexplained variance might be the varying incidence angle resulting from the scanning motion of the laser scanner. The average incidence angle per plot will vary since the plots might be positioned differently with respect to the flight lines. This results in two opposite effects related to the detectability of the vegetation, which change with varying incidence angle: (1) the nadir facing point will

have a smaller footprint and therefore a higher amount of energy per unit area, but (2) the vegetation will be hit vertically resulting in a smaller reflective surface in the direction of the pulse. The combined effect on the detectability will depend on the details of the plant structure. Full waveform laser data combined with the incidence angle could give more insight in this issue.

5.5 *Point density*

For point densities lower than 15 points m^{-2}, the correlation between laser data and field reference data becomes unstable. This is the result of two effects: (1) the accuracy of the DTM decreases due to a less accurate representation of small height variations in the floodplain surface; and (2) there are fewer points to determine the histogram to separate ground points from vegetation points, which renders the labelling more noisy. A solution would be to use a larger area for the determination of the histogram, but this larger area should not include shrubs or trees.

5.6 *Computation of hydrodynamic roughness*

The relations to derive vegetation height and density of non-woody herbaceous vegetation from ALS data could be computed in a moving window or per grid cell of the hydrodynamic model. A few issues arise with the computation of hydrodynamic roughness based on ALS data. Firstly, the relations do not hold for other land cover classes, and should therefore not be applied to other classes. Moreover, single trees within the herbaceous vegetation should be delineated separately, see Morsdorf *et al.* (2004) for details). Secondly, some hydrodynamic models need additional information on flexural rigidity, stem spacing, or bottom roughness (Kouwen and Li 1980, Klopstra *et al.* 1997, Baptist 2005), which cannot be extracted from ALS data directly. However, the product of stem density and flexural rigidity has heen correlated with vegetation height for both growing and dormant grass up to 1 m vegetation height (Kouwen 1988). This relation is not valid for herbaceous vegetation. The bottom roughness, which has a minor effect on the water levels, should be derived from a lookup table. Baptist (2005) provides a model wich can be applied directly using vegetation height and density from ALS data, except for the bottom roughness.

6. Conclusions

With airborne laser scanning, a new tool has become available to quantify vegetation height and density of herbaceous vegetation in senescence, which enables the computation of roughness values for hydrodynamic modelling. Laser scanning provides detailed and accurate estimates of vegetation height and to a lesser extent of vegetation density. Three different vegetation labelling methods were evaluated. The threshold method uses a fixed height above the DTM, the inflection method and the Gaussian method analyse the histogram of the height distribution. The inflection method uses the height above the DTM with the strongest concave-up curvature as a threshold. The Gaussian method explicitly takes the noise of the ground points into account by fitting a Gaussian curve to the ground points. The threshold and the Gaussian method selected fewer points, and are therefore more sensitive to outliers in the height distribution. Vegetation height estimation was most successful using the inflection method for point labelling. The 95 percentile proved the best predictor (R^2=0.74–0.88). However, regression models differed significantly

for datasets that were acquired with different flying height, gain, and laser diode age. The validity range for vegetation height is the height range order of 0.2–2 m. Vegetation density was predicted using the *PI*, which relates vegetation point density to hydrodynamic vegetation density. The *PI* based on the threshold (R^2=0.51) and Gaussian (R^2=0.49) labelling method proved better estimators of vegetation density than the *PI* based on the inflection method (R^2=0.09). This might be caused by difference in reference heights between field and laser data. The validity range for vegetation density is in the order of 0.001–0.7 $m^2 m^{-3}$.

No increase in predictive quality is gained from point densities larger than 15 points m^{-2}. A lower point density might even be possible when larger areas of homogeneous vegetation are present in the study area. Because these herbs in winter are low and thin, the method is sensitive to the combined effect of flying height, gain setting and age of the laser diode. The common factor in these parameters is that they influence the amount of energy at the receiving end of the laser scanner. With increasing energy, the vegetation detection increases too.

We conclude that airborne laser scanning data can be used to map vegetation height and density of senescent floodplain vegetation for floodplain roughness parameterization. Field observations of vegetation structure remain, however, necessary to calibrate the regression models.

Acknowledgements

This work was funded by NWO, the Netherlands Organization for Scientific Research, within the framework of the LOICZ program under contract number 01427004. We would like to thank the Regional Directorate East Netherlands of the Dutch Ministry of Transport, Public Works and Water Management for the free use of all laser altimetry data. Ardis Bollweg and Regine Brügelmann of the AGI are gratefully acknowledged for timely notification of new laser scanning programs, which enabled simultaneous ground truth data collection. Chiel Kollaard and Andries Knotters are thanked for collecting field reference data of surface elevation and vegetation structure. Luc Amoureus of Fugro was very helpful in understanding the differences between the various datasets.

References

BALTSAVIAS, E.P., 1999a, Airborne laser scanning: existing systems and firms and other resources. *ISPRS Journal of Photogrammetry and Remote Sensing*, **64**, pp. 64–198.

BALTSAVIAS, E.P., 1999b, Airborne laser scanning: basic relations and formulas. *ISPRS Journal of Photogrammetry and Remote Sensing*, **54**, pp. 199–214.

BAPTIST, M.J., 2005, Modelling floodplain biogeomorphology, PhD thesis, Delft Technical University, Delft.

BAPTIST, M.J., PENNING, W.E., DUEL, H., SMITS, A.J.M., GEERLING, G.W., VAN DER LEE, G.E.M. and VAN ALPHEN, J.S.L., 2004, Assessment of the effects of cyclic floodplain rejuvenation on flood levels and biodiversity along the Rhine River. *River Research and Applications*, **20**, pp. 285–297.

BRANDTBERG, T., WARNER, T.A., LANDENBERGER, R.E. and MCGRAW, J.B., 2003, Detection and analysis of individual leaf-off tree crowns in small footprint, high sampling density lidar data from the eastern deciduous forest in North America. *Remote Sensing of Environment*, **85**, pp. 290–303.

COBBY, D.M., MASON, D.C. and DAVENPORT, I.J., 2001, Image processing of airborne scanning laser altimetry data for improved river flood modelling. *ISPRS Journal of Photogrammetry and Remote Sensing*, **56**, pp. 121–138.

DARBY, S.E., 1999, Effect of riparian vegetattion on resistance and flood potential. *Journal of Hydraulic Engineering*, **125**, pp. 443–454.

DAVENPORT, I.J., BRADBURY, R.B., ANDERSON, G.R.F., HAYMAN, J.R., KREBS, J.R., MASON, D.C., WILSON, J.D. and VECK, N.J., 2000, Improving bird population models using airborne remote sensing. *International Journal of Remote Sensing*, **21**, pp. 2705–2717.

DUEL, H., BAPTIST, M.J. and PENNING, W.E., 2001, *Cyclic Floodplain Rejuvenation.* NCR publication 14-2001.

EHLERS, M., GÄHLER, M. and JANOWSKY, R., 2003, Automated analysis of ultra high resolution remote sensing data for biotope type mapping: new possibilities and challenges. *ISPRS Journal of Photogrammetry and Remote Sensing*, **57**, pp. 315–326.

FISCHER-ANTZE, T., STOESSER, T., BATES, P. and OLSEN, N.R.B., 2001, 3D numerical modelling of open-channel flow with submerged vegetation. *Journal of Hydraulic Research*, **39**, pp. 303–310.

HILL, R.A., SMITH, G.M., FULLER, R.M. and VEITCH, N., 2002, Landscape modelling using integrated airborne multi-spectral and laser scanning data. *International Journal of Remote Sensing*, **23**, pp. 2327–2334.

HOPKINSON, C., LIM, K., CHASMER, L.E., TREITZ, P., CREED, I.F. and GYNAN, C., 2004, Wetland grass to plantation forest - estimating vegetation height from the standard deviation of lidar frequency distributions. In M. Thies, B. Koch, H. Spiecker and H. Weinacker (Eds), *Laser-scanners for Forest and Landscape Assessment* (Freiburg: Institute for Forest Growth).

HUISING, E.J. and GOMES PEREIRA, L.M., 1998, Errors and accuracy estimates of laser data acquired by various laser scanning systems for topographic applications. *ISPRS Journal of Photogrammetry and Remote Sensing*, **53**, pp. 245–261.

JANSEN, B.J.M. and BACKX, J.J.G.M., 1998, *Ecotope Mapping Rhine Branches—East 1997* (in Dutch). Report no. 98.054 (Lelystad: RIZA).

JESSE, P., 2004, *Hydrodynamic Resistance in Nature Development* (in Dutch). RIZA werkdocument, 2003.124X (Arnhem: RIZA).

KLOPSTRA, D., BARNEVELD, H.J., VAN NOORTWIJK, J.M. and VAN VELZEN, E.H., 1997, Analytical model for hydraulic roughness of submerged vegetation. *27th IAHR Proceedings,* San Francisco, CA, pp. 775–780.

KOUWEN, N., 1988, Field estimation of the biomechenical properties of grass. *Journal of Hydraulic Research*, **26**, pp. 559–568.

KOUWEN, N. and LI, R., 1980, Biomechanics of vegetative channel linings. *Journal of Hydraulics Division*, **106**, pp. 1085–1103.

KRABILL, W., ABDALATI, W., FREDERICK, E., MANIZADE, S., MARTIN, C., SONNTAG, J., SWIFT, R., THOMAS, R., WRIGHT, W. and YUNGEL, J., 2000, Greenland ice sheet: high-elevation balance and peripheral thinning. *Science*, **289**, pp. 428–430.

KRAUS, K. and PFEIFER, N., 1998, Determination of terrain models in wooded areas with airborne laser scanner data. *ISPRS Journal of Photogrammetry and Remote Sensing*, **53**, pp. 193–203.

LEFSKY, M.A., COHEN, W.B., ACKER, S.A., PARKER, G.G., SPIES, T.A. and HARDING, D., 1999, Lidar remote sensing of the canopy structure and biophysical properties of douglas-fir western hemlock forests. *Remote Sensing of Environment*, **70**, pp. 339–361.

LEFSKY, M.A., COHEN, W.B., PARKER, G. and HARDING, D., 2002, Lidar remote sensing for ecosystem studies. *Bioscience*, **52**, pp. 19–30.

LIM, K., TREITZ, P., WULDER, M., ST-ONGE, B. and FLOOD, M., 2003, Lidar remote sensing of forest structure. *Progress in Physical Geography*, **27**, pp. 88–106.

MASON, D.C., COBBY, D.M., HORRIT, M.S. and BATES, P., 2003, Floodplain friction parameterization in two-dimensional river food models using vegetation heights derived from airborne scanning laser altimetry. *Hydrological Processes*, **17**, pp. 1711–1732.

MEANS, J.E., ACKER, S.A., HARDING, D.J., BLAIR, J.B., LEFSKY, M.A., COHEN, W.B., HARMON, M.E. and MCKEE, W.A., 1999, Use of large-footprint scanning airborne lidar to estimate forest stand characteristics in the western cascades of Oregon. *Remote Sensing of Environment*, **67**, pp. 298–308.

MENENTI, M. and RITCHIE, J.C., 1994, Estimation of effective aerodynamic roughness of Walnut Gulch with laser altimeter measurements. *Water Resources Research*, **30**, pp. 1329–1337.

MERTES, L.A.K., 2002, Remote sensing of riverine landscapes. *Freshwater Biology*, **47**, pp. 799–816.

MERTES, L.A.K., DANIEL, D.L., MELACK, J.M., NELSON, B., MARTINELLI, L.A. and FORSBERG, B.R., 1995, Spatial patterns of hydrology, geomorphology, and vegetation on the floodplain of the Amazon River in Brazil from a remote sensing perspective. *Geomorphology*, **13**, pp. 215–232.

MIDDELKOOP, H., and VAN HASELEN, C.O.G. (Eds), 1999, *Twice a River: Rhine and Meuse in the Netherlands.* Report no 99.003 (Arnhem: RIZA).

MORSDORF, F., MEIER, E., KÖTZ, B., ITTEN, K.I., DOBBERTIN, M. and ALLGÖWER, B., 2004, LIDAR-based geometric reconstruction of boreal type forest stands at single tree level for forest and wildland fire management. *Remote Sensing of Environment*, **92**, pp. 353–362.

NAESSET, E., 1997, Estimating timber volume of forest stands using airborne laser scanner data. *Remote Sensing of Environment*, **61**, pp. 246–253.

NAESSET, E., 2002, Predicting forest stand characteristics with airborne scanning laser using a practical two-stage procedure and field data. *Remote Sensing of Environment*, **80**, pp. 88–99.

NAESSET, E., 2004, Effects of different flying altitudes on biophysical stand properties estimated from canopy height and density measured with a small-footprint airborne scanning laser. *Remote Sensing of Environment*, **91**, pp. 243–255.

NAESSET, E. and BJERKNES, K.-O., 2001, Estimating tree heights and number of stems in young forest stands using airborne laser scanner data. *Remote Sensing of Environment*, **78**, pp. 328–340.

NICHOLAS, A.P. and MCLELLAND, S.J., 2004, Computational fluid dynamics modelling of three-dimensional processes on natural river floodplains. *Journal of Hydrodynamic Research*, **42**, pp. 131–143.

NILSSON, M., 1996, Estimating tree heights and stand volume using an airborne lidar system. *Remote Sensing of Environment*, **56**, pp. 1–7.

RINGROSE, S., MATHESON, W. and BOYLE, T., 1988, Differentiation of ecological zones in the Okavango Delta, Botswana by classification and contextural analysis of Landsat MSS data. *Photogrammetric Engineering and Remote Sensing*, **54**, pp. 601–608.

RITCHIE, J.C., MENENTI, M. and WELTZ, M.A., 1996, Measurements of land surface features using an airborne laser altimeter: the HAPEX-Sahel experiment. *International Journal of Remote Sensing*, **17**, pp. 3705–3724.

ROSSO, P.H., USTIN, S.L. and HASTINGS, A., 2005, Mapping marshland vegetation of San Fransisco Bay, California, using hyperspectral data. *International Journal of Remote Sensing*, **26**, pp. 5169–5192.

SCHMIDT, K.S. and SKIDMORE, A.K., 2003, Spectral discrimination of vegetation types in a coastal wetland. *Remote Sensing of Environment*, **85**, pp. 92–108.

SITHOLE, G. and VOSSELMAN, G., 2004, Experimental comparison of filter algorithms for bare-earth extraction from airborne laser scanning point clouds. *ISPRS Journal of Photogrammetry and Remote Sensing*, **59**, pp. 85–101.

STOESSER, T., WILSON, J.D., BATES, P. and DITTRICH, A., 2003, Application of a 3D numerical model to a river with vegetated floodplains. *Journal of Hydroinformatics*, **5**, pp. 99–112.

THOMPSON, A.G., FULLER, R.M. and EASTWOOD, J.A., 1998, Supervised versus unsupervised methods for classification of coasts and river corridors from

airborne remote sensing. *International Journal of Remote Sensing*, **19**, pp. 3423–3431.

VAN DER SANDE, C.J., DE JONG, S.M. and DE ROO, A.P.J., 2003, A segmentation and classification approach of IKONOS-2 imagery for land cover mapping to assist flood risk and flood damage assessment. *International Journal of Applied Earth Observation and Geoinformation*, **4**, pp. 217–229.

VAN STOKKOM, H.T.C., SMITS, A.J.M. and LEUVEN, R.S.E.W., 2005, Flood defense in the Netherlands A new era, a new approach. *Water International*, **30**, pp. 76–87.

VAN VELZEN, E.H., JESSE, P., CORNELISSEN, P. and COOPS, H., 2003, *Flow Friction of Vegetation in Floodplains Part 1* (in Dutch). Report no. 2003.028 (Arnhem: RIZA).

WEHR, A. and LOHR, U., 1999, Airborne laser scanning–an introduction and overview. *ISPRS Journal of Photogrammetry and Remote Sensing*, **54**, pp. 68–82.

WELTZ, M.A., RITCHIE, J.C. and DALE FOX, H., 1994, Comparison of laser and field measurements of vegetation height and canopy cover. *Water Resources Research*, **30**, pp. 1311–1319.

WILSON, C.A.M.E. and HORRIT, M.S., 2002, Measuring flow resistance of submerged grass. *Hydrological Processes*, **16**, pp. 2589–2598.

WONNACOTT, T.H. and WONNACOTT, R.J., 1990, *Introductory Statistics* (Chichester: Wiley).

WOOLARD, J.W. and COLBY, J.D., 2002, Spatial characterization, resolution, and volumetric change of coastal dunes using airborne LIDAR: Cape Hatteras, North Carolina. *Geomorphology*, **48**, pp. 269–287.